Factors to consider in the quest for organic alternatives to hexavalent chromium based corrosion inhibitors

Özkan, Can; Anusuyadevi, Prasaanth Ravi; Visser, Peter; Taheri, Peyman; Mol, Arjan

DOI
10.1016/j.corsci.2025.113183

Publication date
2025

Document Version
Final published version

Published in
Corrosion Science

Corrosion Science 256 (2025) 113183

Contents lists available at ScienceDirect

Corrosion Science

journal homepage: www.elsevier.com/locate/corsci

Factors to consider in the quest for organic alternatives to hexavalent chromium based corrosion inhibitors

Can Özkan [a,*], Prasaanth Ravi Anusuyadevi [a], Peter Visser [b], Peyman Taheri [a], Arjan Mol [a]

[a] Department of Materials Science and Engineering, Delft University of Technology, Mekelweg 2, Delft, 2628 CD, The Netherlands
[b] AkzoNobel, Rijksstraatweg 31, Sassenheim, 2171 AJ, The Netherlands

ARTICLE INFO

Keywords:
Corrosion inhibition
Chromate replacement
Organic molecules
Electrochemistry

ABSTRACT

The search for non-toxic alternatives to hexavalent chromium based corrosion inhibitors requires a comprehensive understanding of the factors critical to effective corrosion protection. Key considerations include the evolution of corrosion inhibition with inhibitor concentrations and exposure times, the inhibition efficacy in the presence and following absence of inhibitors, and the stability of inhibition upon polarisation. In our electrochemical comparison of promising organic molecules with sodium dichromate, we found that even top-performing candidates can lead to premature conclusions if such critical factors are overlooked. While organic molecules can match the inhibition performance of chromates under specific conditions, this can be misleading when considering concentration, time, and polarisation dependent behaviour. Initial high performance can also be deceptive in dynamic environments, as we observed that the inhibition provided by most organic molecules drastically decreases when the inhibitor is absent in the electrolyte. These observations call for broader comprehensive inhibitor robustness studies that take into account factors including time, concentration, stability, and polarisation effects in inhibitor efficacy analysis.

1. Introduction

The use of chromates in corrosion protection for structural materials in aeronautics has been strictly regulated internationally for many years due to health and safety concerns. Despite significant advancements, academia and industry continue to explore various environmentally-friendly and sustainable alternatives to hexavalent chromium (Cr(VI)), which remains the benchmark corrosion inhibitor with a proven track record. According to the EU REACH (Registration, Evaluation, Authorisation, and Restriction of Chemicals) administered by the European Chemicals Agency (ECHA) [1], the use of most chromates was banned in Europe from January 2019 [2].

The development of Cr(VI) alternative corrosion inhibitors is an active area of research, with promising candidates including, but not limited to, lithium [3–5] and rare-earth [6–8] based systems. However, a one-to-one replacement of Cr(VI) pigments remains unlikely, as a recent review suggests [9]. This is due to the Cr(VI) pigments' unique ability to provide multi-functional corrosion protection, including passivation, self-healing, and environmental stability, which is challenging to replicate with a single non-toxic compound. Instead, synergistic systems combining multiple compounds are more viable, with each targeting specific aspects of corrosion prevention.

In this context, organic molecules have emerged as potentially suitable candidates due to their diverse structures and properties. Recent research have highlighted the potential of organic molecules as corrosion inhibitors, with significant progress in understanding structure-performance relationships through studies of related compounds [10], high-throughput screening using optical [11–13], electrochemical [14,15], and spectroscopic methods [13,16,17], and machine-learning models to develop quantitative structure–property relationships [12,13,18–22]. Next to novel data generation, curation of open databases [22–24] and mining research papers through natural language processing [25] have been utilised to effectively search existing literature for potential Cr(VI) replacements.

Despite these advancements, many studies rely on single metrics such as inhibition efficiency or power captured at one timestep and concentration to evaluate inhibition performance [26–29]. While convenient, this approach may not capture all the necessary aspects for identifying next-generation materials. The robustness of the inhibition

* Corresponding author.
E-mail address: c.ozkan@tudelft.nl (C. Özkan).

https://doi.org/10.1016/j.corsci.2025.113183
Received 17 April 2025; Received in revised form 11 July 2025; Accepted 11 July 2025
Available online 29 July 2025

performance under changing environmental conditions is necessary in transforming such molecules into actual problem-solving products, so the understanding of factors resulting in robust corrosion inhibition is most critical. Some of the factors that impact the robustness of the corrosion inhibition are pH, inhibitor concentration, exposure time, as well as the physicochemical and electrochemical stability of the inhibition.

The influence of pH is historically the most well-studied environmental factor. Its effect is twofold: (i) outside the stable pH window where the metal oxide is unstable, corrosion modes might change (e.g. from localised corrosion to a uniform one) and corrosion inhibitors with the right molecular structure and high inhibition efficacy at a mild pH may stop working at a harsh one, (ii) depending on the isoelectric point and pKa values of the inhibitor molecule it might be positively/negatively charged and protonated/deprotonated, changing the surface binding mode and hence its inhibition efficacy [15,30–32]. Despite its critical role, we have highlighted its importance in our previous work, so we focus on other factors in this one [33].

The influence of inhibitor concentration is also a relatively well-studied factor that affects robustness, where until a critical molecule-dependent concentration (often in 1–10 mM range) the inhibition increases, afterwards it plateaus or starts to decrease gradually [34–36]. Manipulating this critical inhibitor concentration is essential for incorporating inhibitors into coatings — when inhibitors leach from a coating matrix onto a defect of a specific size, they have to protect the largest defect area. This distance over which an inhibitor is able to protect a defect effectively is known as the "chemical throwing power", which is crucial in active protective coating design, but not studied for small organic molecules [37].

The influence of time is more sinister, easy to measure but tedious, and most likely for that reason often overlooked. Recent studies highlight that many corrosion inhibitors require a stabilisation period (which can take more than ten hours of exposure) where they gradually form protective layers or reach a stable state, impacting their effectiveness [33,38]. Their efficiency may decline or even reverse over time due to interactions with environmental elements, leading to possible acceleration of corrosion at prolonged exposure. Therefore, continuous or repeated evaluations of inhibitors over time are essential for accurately determining their long-term performance in corrosion control applications [26]. Inhibition performance can also fluctuate due to transient electrochemical changes on metal surfaces, as revealed by Hilbert spectra analysis, where electrochemical noise patterns reflect the evolution of corrosion processes. Time-resolved electrochemical noise measurements can detect early surface transients that indicate the progression from active corrosion to a more inhibited state, emphasising that inhibitors can vary in effectiveness depending on the duration and characteristics of exposure [39].

There is scarcely any work either on influence of physicochemical or on electrochemical stability. A comparison between the benzotriazole and 2-mercaptobenzothiazole molecules with lithium carbonate has shown that all compounds result in effective corrosion inhibition, but the withdrawal of organics from the environment reverses the corrosion inhibition into an uninhibited case. This highlights the need to select the right organic molecules that can sustain inhibition in changing environmental conditions [4]. Polarisation is a widely used method also to analyse such phenomena, but not to understand how inhibited and uninhibited layers change with respect to overpotentials.

In light of these developments, in this study we have analysed key factors that influence the effectiveness of corrosion inhibition, which are crucial for determining whether a molecule is a potentially effective and robust corrosion inhibitor. Building upon our previous work where we screened the electrochemical behaviour of AA2024-T3 substrate exposed to more than 100 organic molecules at 1 mM concentration throughout 24 h [33], we have selected the top-performing non-toxic inhibitors for further study. To highlight the factors critical for corrosion inhibition, we have conducted an electrochemical comparison of ammonium pyrollidinedithiocarbamate and other non-toxic organic molecules with sodium dichromate from different perspectives: the influence of inhibitor concentration, the influence of inhibitor exposure time, the influence of physicochemical stability (inhibitor withdrawal from the environment), and the influence of electrochemical stability (polarisation of the substrate). While corrosion inhibition depends on many variables, including but not limited to temperature, pH, and adsorption kinetics, our focus on these specific factors stems from their often-overlooked importance in translating laboratory results into practical engineering solutions. In particular, physicochemical stability is a critical limitation for the use of organic molecules in self-healing coatings for aerospace applications. The results of this study are expected to steer inhibition efficiency and robustness studies and facilitate the development of Cr(VI) replacement organic molecules by unveiling the nature of corrosion inhibition at different and varying conditions.

2. Experimental

2.1. Sample preparation

2 mm thick AA2024-T3 sheets were purchased from Salomon's Metalen B.V., the Netherlands, to use as the substrates for the electrochemical experiments. After cut into 20 mm × 20 mm samples with an automatic shear cutting machine, samples were ground with progressively finer grits of 320, 800, 1200, 2000 and 4000 with a rotating plate sander under a running water. The resulting ground samples were then ultrasonically cleaned in isopropanol for 15 min and subsequently dried with compressed air.

2.2. Electrolytes

The inhibitor selection reasoning was based on a process of elimination building on our previous inhibitor screening study [33]. The chosen inhibitors were the non-toxic molecules with the highest corrosion inhibition efficiencies. 4-mercaptobenzoic acid showed highest performance in our previous work, however it was already insoluble at 1 mM concentrations, which made further work on inhibitor concentration studies at higher concentrations challenging. A similar solubility challenge was also present for the second one in the ranking of our previous work, 2-mercaptopyrimidine. That left ammonium pyrollidinedithiocarbamate and 3-amino-1,2,4-triazole-5-thiol for further study, which were ranked at positions 3 and 5 (after sodium mercaptoacetate which was not considered for this work due to its toxicity).

Electrochemical measurements were conducted at room temperature in open-to-air 0.1M NaCl solutions, with (or without) the added 1 mM inhibitor candidates: 3-amino-1,2,4-triazole-5-thiol, 2-mercaptopyridine, 2-mercaptopyrimidine, 4-mercaptobenzoic acid, ammonium pyrollidinedithiocarbamate, sodium diethyldithiocarbamate. Sodium dichromate solutions were prepared by first making a 10 mM stock solution with sodium dichromate dihydrate. This solution was diluted with pure water and mixed with NaCl to prepare final solutions for electrochemical experiments. For concentration experiments additional electrolytes were prepared in the range of 0.05 to 10 mM concentrations. The basis salt solutions without the addition of inhibitors (pH 5.9) were prepared with NaCl powder with Milli-Q pure water (15.0 MΩ cm resistance at 25 °C). For cyclic voltammetry measurements, 0.1M Na_2SO_4 solution with 1 mM ammonium pyrollidinedithiocarbamate or 3-amino-1,2,4-triazole-5-thiol electrolytes were prepared. No additional compounds were added to modify the pH and/or increase the solubility of inhibitors. All chemicals were obtained from Sigma-Aldrich, except for sodium chloride (J.T. Baker) and 3-amino-5-mercapto −1,2,4-triazole (Alfa-Aesar).

2.3. Electrochemical experiments

The electrochemical measurements consisted of the following techniques: open circuit potential (OCP) observation, linear polarisation resistance (LPR), electrochemical impedance spectroscopy (EIS) potentiodynamic polarisation (PDP), and cyclic voltammetry (CV). The experiments were performed in a flat three-electrode electrochemical cell (Corrtest Instruments, China) where the sample was the working, platinum mesh was the counter, and Ag|AgCl (saturated KCl) was the reference electrode. The exposed surface area was 0.785 cm^2, covered by a 250 ml electrolyte volume. Biologic VSP-300 multichannel potentiostats were used to control the electrochemical measurements through EC-Lab software (version 11.33, Biologic, France). Only for sodium dichromate experiments Gamry E1010 potentiostats with Gamry software were used. The electrochemical behaviour of background uninhibited cases were compared to make sure the results between different potentiostats matched.

All electrochemical experiments were repeated at least three times per inhibitor to confirm the reproducibility of the experiments. All potentials presented in this work refer to the Ag|AgCl (saturated KCl) reference potentials unless mentioned differently.

2.3.1. Influence of inhibitor concentration

Inhibitor concentrations were varied from 0.05 to 10 mM for sodium dichromate or ammonium pyrollidinedithiocarbamate dissolved in 0.1M NaCl electrolytes. To check the influence of inhibitor concentration, separate anodic and cathodic potentiodynamic polarisation curves were recorded after 6 h of OCP in a single sweep with a scan rate of 0.5 mV/s from −(+) 10 mV to +(−) 500 mV potentials with respect to the OCP values. Linear polarisation resistance values were calculated from the initial ∓ (±) 10 mV parts of the scans.

2.3.2. Influence of time

To check the influence of time, potentials were scanned from −10 mV vs. OCP to +10 mV vs. OCP at a rate of 0.5 mV/s every 10 min for 24 h. OCP was observed in between the scans. A linear fit was applied to the observed potential vs. current density plots to obtain the polarisation resistance (R_p) values. At the 2nd and 24th hour, EIS measurements were conducted. A sinusoidal AC perturbation with a peak-to-peak amplitude of 10 mV was applied from 10 kHz to 10 mHz frequency range with 10 frequency point per logarithmic decade. Measurement was repeated 3 times per frequency point. 10 min of OCP was observed between LPR and EIS experiments.

2.3.3. Influence of physicochemical stability

To check the influence of physicochemical stability, electrochemical experiments were carried out in inhibitor-containing solutions for the first day, and inhibitor-absent solutions for the last 3 days. The first 24 h of electrochemical experiments were conducted in 1 mM inhibitors dissolved in 0.1M NaCl solutions. Afterwards the electrolyte was poured out, the electrochemical cell was rinsed, and a new electrolyte containing only 0.1M NaCl solutions was used for the rest of the electrochemical experiments.

The electrochemical investigations were initialised after observing the OCP. LPR was measured over a potential range of ±10 mV with a scan rate of 0.5 mV/s after 1, 2, 6 h and afterwards every 6 h. OCP was observed in between LPR measurements. EIS measurements were conducted directly after LPR measurements every 6 h,in the same manner as discussed previously. The selected data from EIS were quantified with equivalent electrical circuit fitting with the Zview software (v3.5 h, Charlottesville, USA).

2.3.4. Influence of electrochemical stability

After observing OCP for 1 h under exposure to 0.1M Na_2SO_4 with 1 mM ammonium pyrollidinedithiocarbamate or 3-amino-1,2,4-triazole-5-thiol, samples were scanned with 10 mV/s scan rate in a cyclic voltammetry fashion from 0.7 to −1.2 V vs. Ag/AgCl(saturated KCl). The scan was repeated 5 times, but only the first 2 are presented here as the last 4 cycles resulted in the same behaviour.

3. Results and discussion

3.1. Influence of inhibitor concentration

Fig. 1 plots the anodic and cathodic polarisation curves of AA2024-T3 exposed to 0.1M NaCl electrolytes with sodium dichromate or ammonium pyrollidinedithiocarbamate at different concentrations. Fig. 2 summarises the linear polarisation resistance (R_{LPR}) and corrosion potential (E_{corr}) values obtained from the scans of Fig. 1.

From Figs 1(a) and (b) and Fig. 2 potential trends we observe that the addition of sodium dichromate, even as little as 0.05 mM, shifted corrosion potentials to more negative potential values of −50 to −70 mVs. Further concentration increases did not result in further changes in the corrosion potentials. As a result, active pitting behaviour (a rapid increase in anodic corrosion current densities at corrosion potentials) of uninhibited case changed with dichromate additions. For dichromate additions of less than 1 mM, even though pitting occurred at uninhibited corrosion potentials, shift of corrosion potentials resulted in a larger stable potential range. For dichromate additions of more than 1 mM, an approximately 20 mV extra range of Tafel behaviour appeared, due to the 20 mV positively shifted pitting potentials. This suggests further stabilisation of pits higher than this 1 mM critical concentration. Fig. 1(a) shows that increased dichromate concentrations decreased anodic current densities. 0.05 mM dichromate addition decreased corrosion current by an order of magnitude, and this decrease only continued with an increase in concentration. Cathodic curves of Fig. 1(b) showed more than 2 orders of magnitude current density decrease with the addition of 0.05 mM dichromate, however no additional decrease in current densities were observed with an increase in dichromate concentration. Cathodic curves showed similar behaviour rather independent of the dichromate concentration. This suggests cathodic inhibition was complete starting from as little as 0.05 mM dichromate concentration. This behaviour aligned with trends observed in R_{LPR} values plotted in Fig. 2. The addition of sodium dichromate increased R_{LPR} (in kOhm cm^2) values to 256 ± 210 for 0.05 mM, up to a maximum of 428 ± 32 for 5 mM concentration. The standard deviation of measurements decreased with increasing concentrations with the exception of the maximum measured concentration 10 mM, and the mean values with their deviations overlapped between 0.1 – 10 mM concentrations.

Inhibition of corrosion by Cr(VI) compounds is due to their ability to adsorb onto the metal/oxide surfaces irreversibly, subsequently get reduced to form inert hydrophobic Cr(III) oxide barrier films, with retained releasable Cr(VI) reservoirs. Non-reduced Cr(VI) oxoanion adsorbtion on Al-oxides modifies the zeta potential, discouraging adsorption of corrosive ions such as chlorides that promote dissolution and destabilisation of the protective oxide films, further inhibiting pitting [40–42]. A 0.05 mM chromate concentration was found to be sufficient for the formation of such chemical chromate conversion films: Cr(VI) - Cr(III) mixed oxides which primarily suppress the cathodic oxygen reduction reaction (ORR) rate and inhibit localised corrosion initiation [43,44]. For AA2024-T3 specifically, the chemical conversion layer thoroughly reduces corrosion activity at both the cathodic sites such as Cu-rich θ- and dealloyed S-phase intermetallic particles, and the Al matrix with the anodic intermetallics within [45,46]. Based on this literature, we can infer that in our experiments 0.05 mM dichromate concentration was sufficient to form a barrier film that suppresses cathodic reactions, which did not change further with an increase in dichromate concentration. Meanwhile, further increase in dichromate concentration increased available Cr(VI) oxoanion ready to adsorb and suppress the localised pitting activity, which would explain the increased potentials required for pitting initiation, and consistent decrease of anodic current densities with increasing dichromate concentrations.

Addition of ammonium pyrollidinedithiocarbamate showed completely different trends. Despite the constant pH values around 6.0–6.5

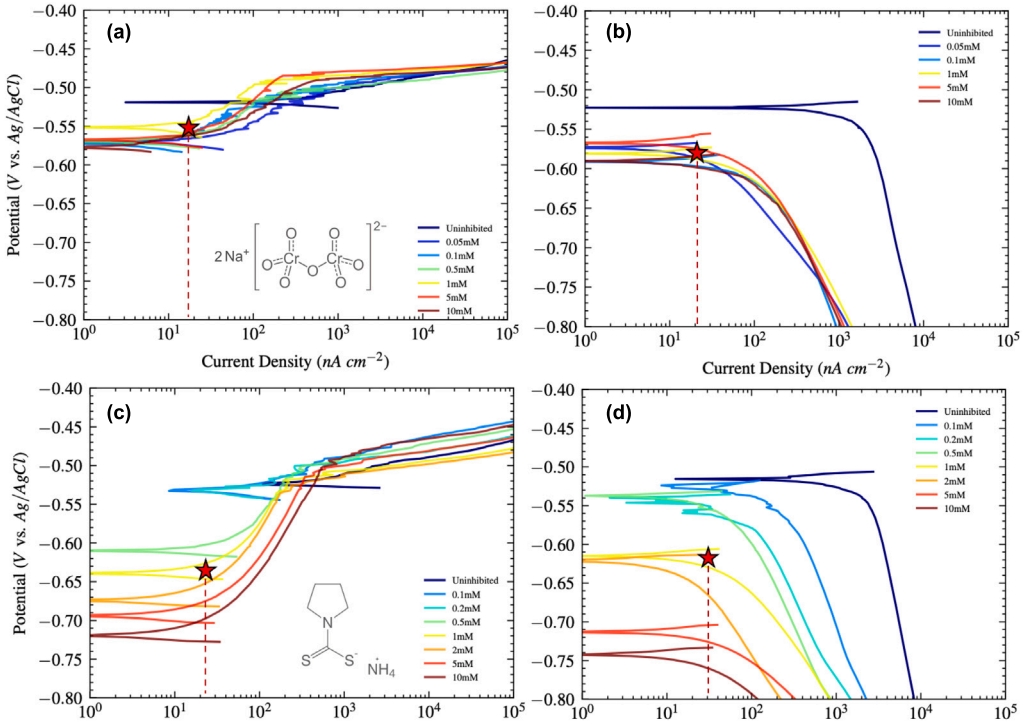

Fig. 1. Potentiodynamic polarisation curves of AA2024-T3 exposed to 0.1M NaCl electrolytes with varying inhibitor concentrations: (a) sodium dichromate anodic polarisation, (b) sodium dichromate cathodic polarisation, (c) ammonium pyrollidinedithiocarbamate anodic polarisation, (d) ammonium pyrollidinedithiocarbamate cathodic polarisation. Red stars indicate corrosion potentials and currents at 1 mM concentrations.

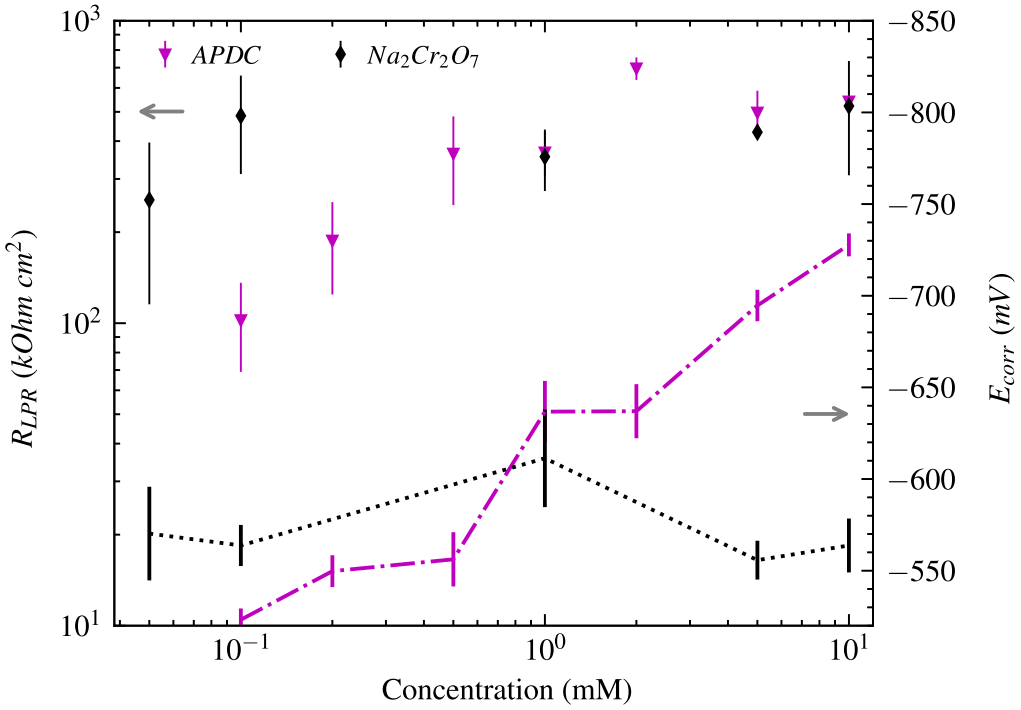

Fig. 2. Influence of concentration on polarisation resistance and potential values for ammonium pyrollidinedithiocarbamate ($APDC$) and sodium dichromate ($Na_2Cr_2O_7$). Linear polarisation resistance (R_{LPR}) and corrosion potential (E_{corr}) values obtained from the initial parts of the anodic (cathodic) scans for ∓ (±) 10 mV range. Top markers correspond to the R_{LPR} scale shown on the left axis, bottom lines correspond to the E_{corr} values shown on the right axis. Values corresponding to the bottom plot border (10 kOhm cm^2 and -520 mV Ag/AgCl) correspond to the mean uninhibited case.

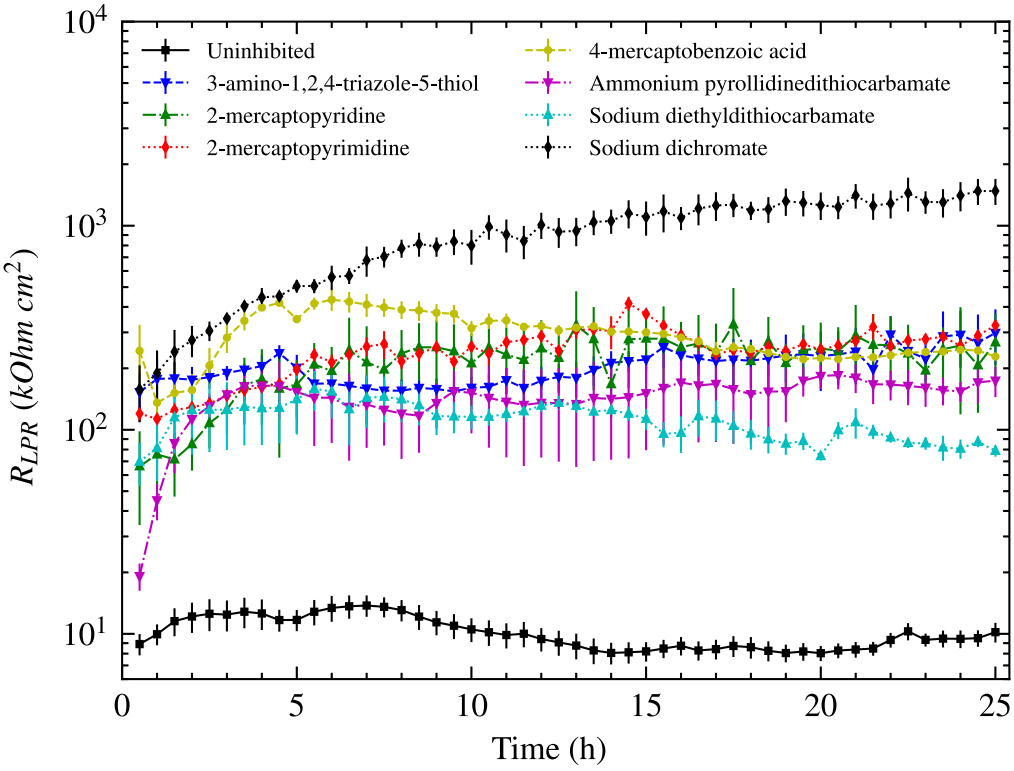

Fig. 3. Influence of time on the linear polarisation resistance (R_{LPR}) of AA2024-T3 in the presence (and absence) of 1 mM corrosion inhibitors.

at all concentrations, the electrochemical potentials changed significantly. Figs. 1c and 1d show that corrosion potentials systematically shifted to more negative potentials with increases in concentration. This resulted in a passive range that became larger and larger with inhibitor concentration, which is expected to limit the localised electrochemical activity. The current densities of both anodic and cathodic curves decreased until 2 mM concentration, after which they started to increase. This is consistent with R_{LPR} values plotted in Fig. 2, where ammonium pyrollidinedithiocarbamate addition increased R_{LPR} (in kOhm cm^2) values to 102 ± 50 for 0.1 mM, up to a maximum of 697 ± 89 for 2 mM, and decreased to 498 ± 132 for 5 mM concentrations. This plateauing or decrease in performance after a certain critical inhibitor concentration was likely due to more disordered self-assembled monolayers [47], which has previously been attributed to surface saturation with adsorbed molecules or self-micelle formation [35,48,49]. The decrease in current densities of both anodic and cathodic curves suggests an inhibitive film formed both on anodic Al matrix and anodic/cathodic intermetallics, the majority of which contain Cu [50]. Inhibiting the dealloying of Cu-rich intermetallics is critical in limiting the overall corrosion of AA2024-T3, as they are the main microgalvanic driving force for the electrochemical reactions. Previous studies confirm that ammonium pyrollidinedithiocarbamate can inhibit Cu by decreasing the active surface area and raising the charge transfer resistance through formation of an amorphous inhibitive film [51].

Initial comparison of concentration influence of both inhibitors seems to suggest that electrochemical performance of ammonium pyrollidinedithiocarbamate is on par with sodium dichromate for the 1–10 mM concentration range. It would seem as if our research has finally found the replacement for hexavalent chromium compounds. However is that really the case? For this end, the next section explores the behaviour of time on the electrochemical behaviour.

3.2. Influence of time

Fig. 3 plots the polarisation resistance (R_{LPR}) values throughout time for the first 24 h. In addition to ammonium pyrrolidinedithiocarbamate, we tested 5 other non-toxic organic molecules that had shown promising corrosion inhibition properties during our previous screening [33]. R_{LPR} values of the uninhibited case were relatively constant around 10 ± 3 kOhm cm^2 throughout the first day. The organic molecules increased the R_{LPR} values in the range of 78 ± 9 to 325 ± 10 kOhm cm^2, but not immediately. It is observed that organic molecules require some time to stabilise and reach their peak polarisation resistance R_{LPR} values, which was around 6 h. After that point, R_{LPR} values reached a plateau and did not change significantly anymore. On the other hand, polarisation resistance originating from the sodium dichromate kept increasing throughout the whole day, up to 1479 ± 431 kOhm cm^2.

Looking back on the concentration experiments presented in the previous section, we can explain the comparable behaviour of sodium dichromate with the organic molecules observed after 6 h. Whereas the ratio of polarisation resistance values of sodium dichromate and ammonium pyrollidinedithiocarbamate was around 2–3 around the 6-hour mark, which matches which trends from last section, this value increases to 8–10 at the 24th hour. This corresponds to inhibition efficiencies of 87%–97% for organics, while sodium dichromate reached an inhibition efficiency of more than 99%. This shows that if we only look at the time-step of 6th hour, or any other single time-step for that matter, we come to the wrong conclusion about the behaviour. The gradual initial increase culminating in a plateau of polarisation resistance for the adsorption of organic molecules, and continuous development of the protective chromium oxide films highlight the time-sensitive nature of the corrosion inhibition, and the critical need for time-resolved measurements. The importance of time-resolved electrochemical measurements were highlighted before in a previous study [26]; here we once again underline that without time-resolved measurements, it is unlikely to have a correct efficacy assessment of the next-generation chromate replacement compounds.

3.3. Influence of physicochemical stability

Sustaining corrosion inhibition in changing environments is as important as sustaining corrosion inhibition throughout time. It is critical

to keep corrosion inhibition going in dynamic conditions, especially in the widely-changing conditions observed for aerospace alloys: dry-wet cycles, temperature fluctuations, among others [52]. We name the sustained inhibition in the changing environmental conditions *physicochemical stability* of the inhibitor, which in previous papers were also called irreversibility of the inhibition [4].

To check the behaviour of physicochemical stability we have observed electrochemical impedance response of selected high performing organic corrosion inhibitors and sodium dichromate at 1 mM concentrations. Electrochemical impedance spectroscopy measurements were first performed in the presence of inhibitors after 12, 18 and 24 h of exposure, afterwards substrates were exposed to electrolytes without any inhibitors and electrochemical impedance spectra were acquired for every 6 h after the 12th hour for 3 days.

Fig. 4(a) shows the resulting impedance modulus plots for the final measurements before and after electrolyte switch. Filled markers represent the case in the presence of inhibitors, and empty markers represent the case of the following absence of inhibitors. It is visible from the plots that the addition of inhibitors consistently increases the impedance modulus values. Sodium dichromate results in the largest impedance modulus increase. After changing the electrolytes, impedance modulus of all systems decrease significantly: the impedance modulus of all organic inhibitor systems except for 3-amino-1,2,4-triazole-5-thiol drop down to the uninhibited level, while sodium dichromate shows significantly higher modulus values. Even after the electrolyte exchange the impedance modulus values of sodium dichromate only drop down to the levels of organic inhibitor present systems. Fig. 4(b) shows the mean drop in impedance modulus values at 10^{-2} Hz converted into inhibition power. It is clear that apart from 3-amino-1,2,4-triazole-5-thiol, all organic molecules stop providing corrosion inhibition if they are not sustained in the environment. In this case 3-amino-1,2,4-triazole-5-thiol loses most of its inhibition as well – 74% of the initial inhibition power is lost – but it is not completely gone, resulting in a quasi-reversible corrosion inhibition behaviour. For comparison, sodium dichromate only loses 39% of its original inhibition power.

Fig. 5 focuses on sodium dichromate, ammonium pyrollidinedithiocarbamate, and 3-amino-1,2,4-triazole-5-thiol. 3-amino-1,2,4-triazole-5-thiol still sustained some impedance modulus increase after the electrolyte switch. This is a key quality for stable and irreversible corrosion inhibition, as the low-frequency impedance determines the total retained corrosion resistance of the system [26]. As the frequency tends towards infinity, the impedance modulus magnitude tends towards the resistance of the electrolyte; as the frequency tends towards zero, capacitive contributions disappear and the impedance modulus magnitude tends towards the total impedance coming from the electrolyte, inhibitor, and charge transfer [53,54]. Similar impedance behaviour between samples above 10^3 Hz stemmed from electrolyte impedances, resulting in similar impedance modulus values. The phase angle values became more negative as the frequency decreased: the more the corresponding impedance modulus, the steeper the phase angle decrease. This was the result of the capacitive dielectric formed on the substrate through oxide and/or adsorbed inhibitors. Related impedance modulus increase and more capacitive behaviour between 10^{-1} - 10^3 Hz stemmed from the electron transfer processes of the inhibitor-oxide/metal surface [55]. The behaviour in further lower frequencies corresponds to either resistive charge transfer processes where phase angle approaches 0, or otherwise mass-transfer limited diffusion processes where phase angle approaches -45 [53,54]. The slowest time constant at lower frequencies ($\omega_{char} \sim 1/\tau = 1/RC$), which is the measure of how quickly the system responds to external changes in voltage and current [56], appeared at lower frequencies in the presence of inhibitors, which means the time constant has increased. This increase meant slowing down the electrochemical system, either through an increase in resistance or capacitance, through limiting charge transfer or diffusion. After the electrolyte switch time constants decreased again

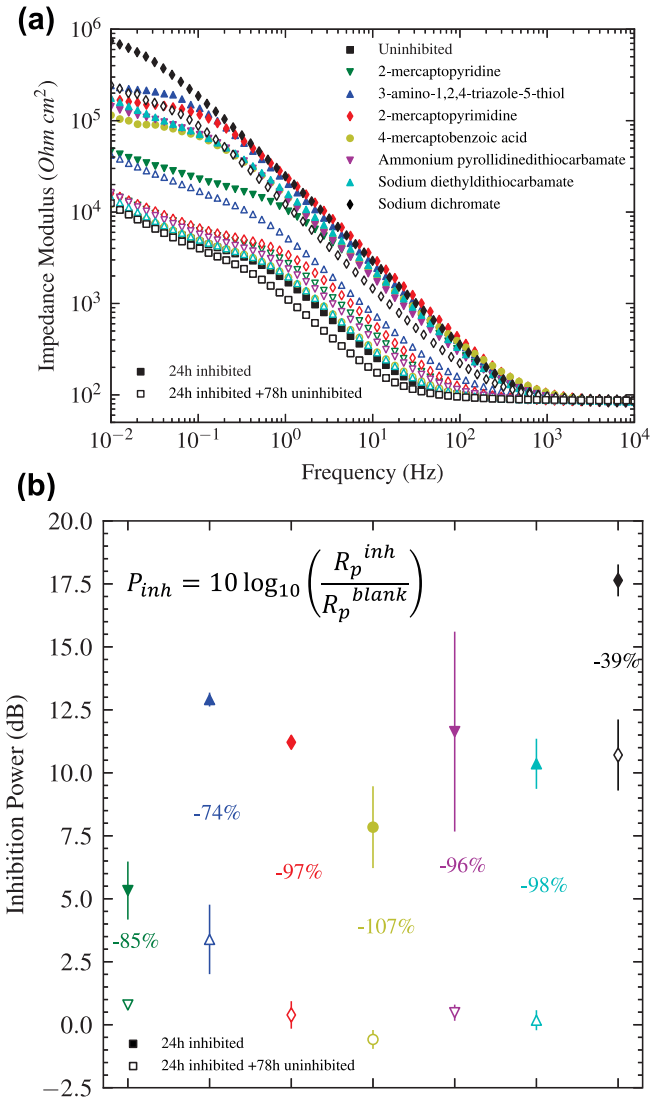

Fig. 4. Influence of presence and subsequent absence of corrosion inhibitors on electrochemical behaviour. Filled markers represent the electrochemical impedance spectroscopy response before electrolyte exchange, while empty markers indicate the response after exchange. (a) Impedance modulus spectra for organic inhibitors. (b) Comparison of the impedance modulus at 10^{-2} Hz, converted to inhibition power (P_{inh}), before and after electrolyte exchange. The percentage reduction in original protection is indicated between the markers. Both subplots share the same legends.

for all systems. The low frequency phase angles of uninhibited and ammonium pyrollidinedithiocarbamate samples approached towards −45° (also apparent as a low-frequency slope of 1 in Nyquist visualisation, shown in Supplementary Information), which suggests a diffusion-limited response. For others that was not the case. These suggest that a complete or quasi-reversal to the non-protected behaviour develops in the absence of a sustained inhibitor in the environment. The difference most likely originates from the different surface bonding behaviour of organic molecules. The inhibitors that maintained their effectiveness formed stable surface complexes or stabilised oxide layers that resisted their removal and/or dissolution of the substrate after the electrolyte switch.

To quantify inhibitors' electrochemical response, a modified Randles circuit shown in Fig. 5 inset is used as an equivalent electrical circuit to fit the spectra. The chosen circuit with two time constants was used to model the physics of the metal electrode covered with

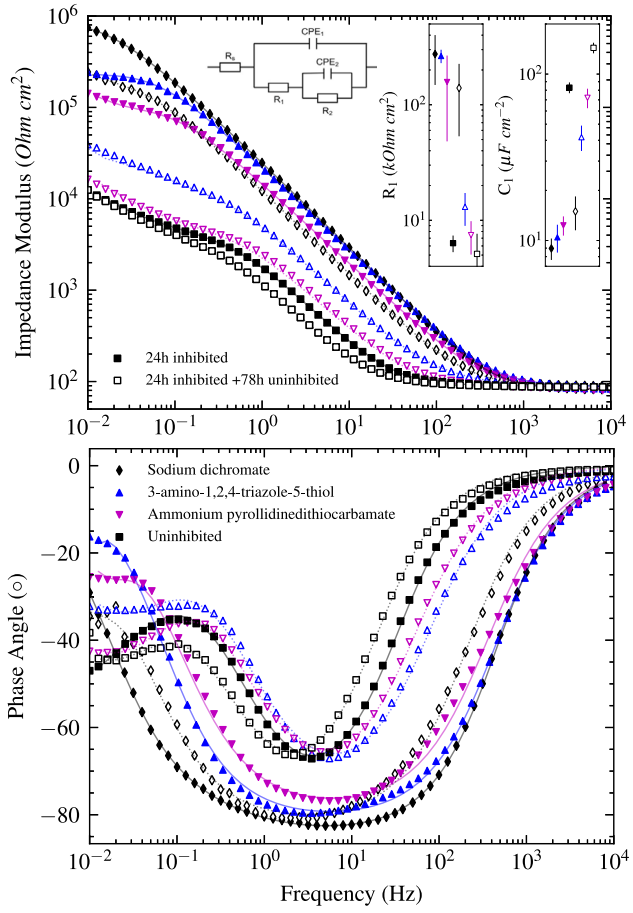

Fig. 5. Impedance modulus and phase angle plots with equivalent circuit fits demonstrating the influence of presence and subsequent absence of corrosion inhibitors on electrochemical impedance spectroscopy response. Selected equivalent circuit and fit values relevant to the inhibition shown in the inset.

an imperfect overlaying inhibitor layer. This is a widely used equivalent circuit fit used for modelling the impedance of an electrode coated by a thick dielectric layer with pores exposing the electrode to the electrolyte [53,57–59]. In this fit R_s, R_1 and CPE_1, R_2, CPE_2 corresponded to the electrolyte resistance, protective film resistance (through adsorbed molecules and/or passive film) and its associated capacitance, charge transfer resistance and the double layer capacitance, respectively. Constant phase elements (CPE) are employed instead of capacitors due to the deviation from the ideal capacitive behaviour. Capacitance of the constant phase elements were calculated according to the Hsu–Mansfeld approach [60]:

$$C = R^{\frac{1-n}{n}} Q^{\frac{1}{n}} \tag{1}$$

where C is the capacitance, R the resistance, Q is the magnitude of the CPE associated with its capacitance, and n an empirical constant, taking values between 0 and 1 (1 represents the case for the ideal capacitor, 0 the ideal resistor, and in between values the non-ideal capacitive responses). The calculated equivalent resistance and capacitance values related to the presence/absence of inhibitors are plotted as an inset of Fig. 5. Resistance values increased up to 50-fold in the presence of inhibitors. The capacitance values showed an order of magnitude decrease in the presence of inhibitors as well. Through the relationship [53]:

$$C = \frac{\varepsilon_0 \varepsilon}{d} \tag{2}$$

where C is the capacitance, ε_0 the vacuum permittivity, ε is the relative permittivity, and d the thickness of the dielectric field responsible for capacitive behaviour, it can be argued that corrosion inhibitors either created a steric hindrance through a thicker barrier film, or decreased the relative permittivity of the surface. After the electrolyte change the resistance values had a sharp decline: dichromate resistance dropped to half of its original value but stayed strongly inhibitive, 3-amino-1,2,4-triazole-5-thiol dropped to a fraction of its original gained inhibition and showed around 65% inhibition efficiency, whereas ammonium pyrollidinedithiocarbamate lost all inhibition. Trends were similar for capacitance: capacitance of dichromate doubled, 3-amino-1,2,4-triazole-5-thiol quadrupled, whereas ammonium pyrollidinedithiocarbamate returned to uninhibited values. Doubling of capacitances for the uninhibited case is most likely resulting from the growth of the Al-oxide under the 3-day electrolyte exposure.

Fig. 6 plots the evolution of impedance modulus values measured at 10^{-2} Hz frequency to understand the stability of inhibitor systems through time. Although being based on a simplification since the low-frequency impedance modulus includes contributions from the oxide film resistance, the charge transfer resistance, and often from the diffusion-controlled processes — it has been shown that the impedance modulus values observed at 10^{-2} Hz frequency effectively represent the corrosion resistance of the inhibitor–substrate interface [61].

It is observed that the electrochemical behaviour of almost all samples returns to the uninhibited performance 60 h after the inhibitor removal. 3-amino-1,2,4-triazole-5-thiol sustains its – albeit decreased – protection at least for 3 days after the electrolyte exchange, but all other organics completely lose their protection. Dichromate sustains its original protection for a long time, and even after 3 days measured impedance modulus is more than 5-fold the impedance modulus of the best organic corrosion inhibitor.

These observations suggest that corrosion inhibition gained through organic molecules is lost for almost every organic system if the molecule is not sustained in the environment. Despite the initial inhibition, the majority of the tested organic molecules have reversible bonds that limit their inhibition performance and applicability in dynamic environments. Best-performing inhibitors were not necessarily more irreversible or had a higher performance after electrolyte change. 3-amino-1,2,4-triazole-5-thiol provides a quasi-reversible corrosion inhibition, possibly through more permanent bonds formed with some of the intermetallics instead of the Al substrate. Sodium dichromate showed the best inhibition performance before and after the electrolyte exchange, but it also showed a significant decrease in inhibition. However, even when the dichromate was absent afterwards, the inhibition was better than the best organic inhibitor tested in this study.

3.4. Influence of electrochemical stability

Corrosion inhibition must be sustained in a wide range of electrochemical potentials. In the vicinity of the localised galvanic couples, such as pitting corrosion cells of AA2024-T3 [46], open circuit potential is different because as the electrochemical corrosion reactions proceed anodic areas become more acidic while cathodic areas become more basic, both destabilising the oxide of aluminium alloys. Ensuring corrosion inhibition in a wide range of potentials minimises such microgalvanic interactions, which we here label as the *electrochemical stability*.

Presence of chromates were previously shown to suppress current densities in a wide potential range and specifically Cu oxidation [17,62], providing electrochemical stability, but such studies on organics are often missing from the literature. To check the behaviour of electrochemical stability of organic molecules we have performed cyclic voltammetry measurements. In total 5 cycles were recorded, but no significant change in electrochemical behaviour is observed so only the first 2 cycles are plotted in Fig. 7. Cycles are initiated from positive

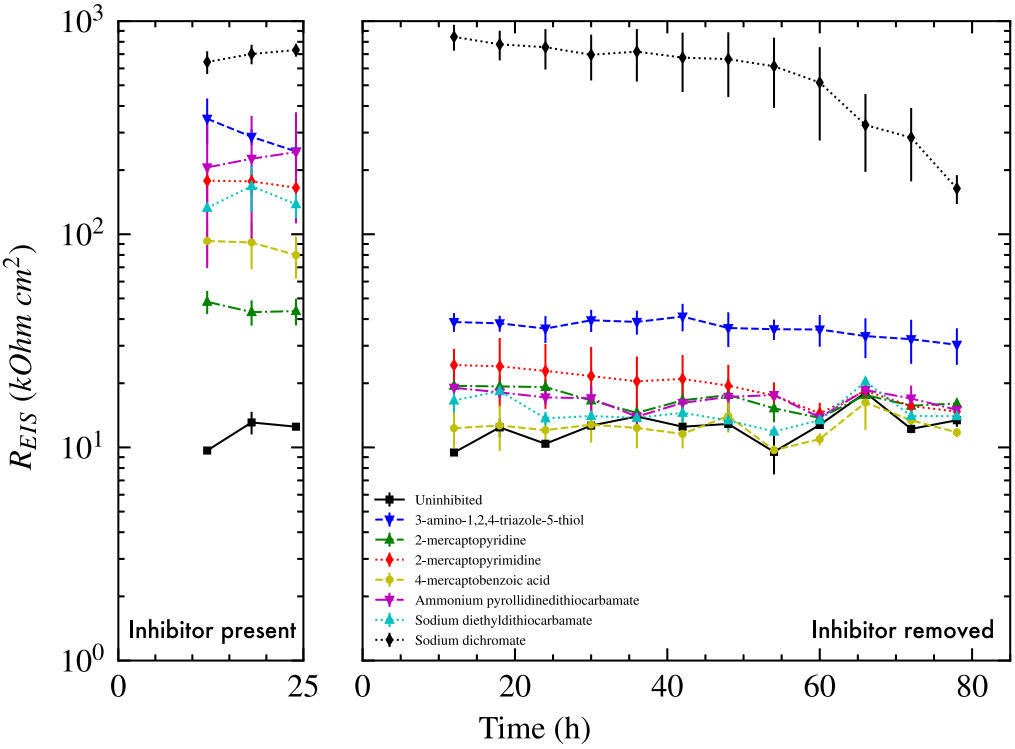

Fig. 6. Evolution of impedance modulus values measured at 10^{-2} Hz frequency.

towards the negative potentials, with the hypothesis that initially the inhibitors would form self-assembled monolayers in the first hour of exposure, then they would be forcibly desorbed throughout the scan to the negative potentials (assuming deprotonated negatively charged molecules, which is justified given the low pKa trend of mercaptans [63]), then electrosorbed [64] again to the aluminium surface with the positive scan. The first and second scan would show the difference between self assembled monolayer and electrosorption behaviour.

On the scan towards negative potentials, for the uninhibited case a peak appears around −0.55 V, which shifts to −0.65 V for the second cycle. The onset values of these peaks are typical for diffusion limited oxygen reduction reaction (ORR), which extend up to around −1.1 V where hydrogen evolution reaction appears as a sharp increase in cathodic current densities [65]. ORR is dependent on the surface properties and composition — because of the surface modifications to Al (hydr)oxide during the first scan, the ORR onset shifts to more negative potentials and result in higher peak current densities. Looking at the results for organic inhibitors during the first scan, ORR is partially suppressed for ammonium pyrollidinedithiocarbamate, and completely suppressed for 3-amino-1,2,4-triazole-5-thiol after the self-assembly process of the adsorbed organic layers. After the second cycle, the current densities decrease even more and the peak of ammonium pyrollidinedithiocarbamate present in the first scan disappears, suggesting increased inhibition through the electrosorption.

On the scan back towards positive potentials, for the uninhibited case a peak appears around −50 mV. The position and magnitude of this peak matches very well with literature where cyclic voltammetry and glow discharge mass spectrometry (GDMS) was used on AA2024 [66], with which this peak was attributed to surface enrichment with Cu due to the anodic Cu oxidation reactions:

$$2Cu + H_2O \rightarrow Cu_2O + 2H^+ + 2e^- \quad (3)$$

$$Cu_2O + H_2O \rightarrow 2CuO + 2H^+ + 2e^- \quad (4)$$

For the uninhibited case both cycles had this peak, which was completely suppressed in the presence of organic inhibitors. This would mean that organic inhibitors are successful in preventing surface enrichment with Cu, in both self-assembled and electrosorbed form, which is a critical corrosion initiation mechanism for Al–Cu alloys. Both molecules conveyed stable inhibition in a wide potential range.

4. Conclusions

In order to support the quest for promising non-toxic alternatives to hexavalent chromium based inhibitors, we have to be aware of how the corrosion inhibition evolves with inhibitor concentration and measurement time, and whether it is stable in the presence/absence of the inhibitor molecule in a wide potential range. Here we show that even after screening more than 100 organic molecules experimentally, the best-performing molecules from the screening can tempt us to jump to premature conclusions. When not taking different corrosion inhibition critical factors such as time, concentration and physical/electrochemical stability into consideration, conclusive remarks about final performance cannot be drawn. We have observed that at 1 mM concentrations some organic compounds do offer comparable inhibition to sodium dichromate around the 6-hour mark, but afterwards performance of chromate keeps increasing throughout the first day whereas organics reach a stable plateau. Despite the initial inhibition, the majority of the tested organic molecules have reversible bonds that limit their inhibition performance and applicability in dynamic environments where a constant inhibitor reservoir is not present. Compared to weaker inhibitors, best-performing inhibitors were neither necessarily more physically stable and irreversible, nor had a higher performance after removal from the electrolyte. On the other hand, when the organic molecules are sustained in the environment they can offer corrosion inhibition away from the open circuit potential for a wide potential range, and can suppress both Cu oxidation and oxygen reduction reactions. Some minority molecules show that quasi-stable corrosion inhibition is possible with small organic molecules — meaning long-term (studied up to 3-days in this work) stable barrier properties are possible even when the molecules are withdrawn from the environment, albeit at a lower inhibition.

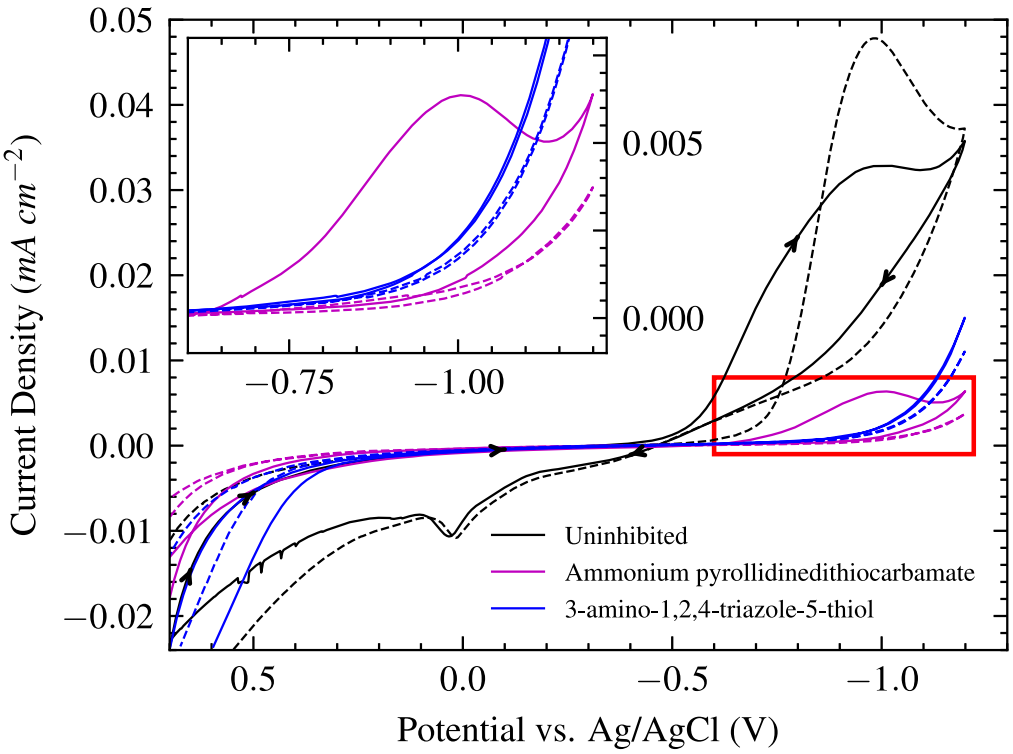

Fig. 7. Cyclic voltammetry measurements of AA2024-T3 in the presence (and absence) of 1 mM corrosion inhibitors. Solid lines show the first, dashed lines show the second cycle. Inset figure is the close-up of the red framed area in the cathodic overpotential region.

CRediT authorship contribution statement

Can Özkan: Writing – original draft, Visualization, Methodology, Investigation, Formal analysis, Conceptualization. **Prasaanth Ravi Anusuyadevi:** Writing – review & editing. **Peter Visser:** Writing – review & editing, Resources. **Peyman Taheri:** Writing – review & editing, Supervision. **Arjan Mol:** Writing – review & editing, Supervision, Resources.

Declaration of competing interest

The authors declare that they have no known competing financial interests or personal relationships that could have appeared to influence the work reported in this paper.

Acknowledgements

This work is a part of the VIPCOAT project (Virtual Open Innovation Platform for Active Protective Coatings Guided by Modelling and Optimisation) funded by Horizon 2020 research and innovation programme of the European Union by grant agreement no. 952903.

Appendix A. Supplementary data

Supplementary material related to this article can be found online at https://doi.org/10.1016/j.corsci.2025.113183.

Data availability

Data will be made available on request.

References

[1] The European Parliament and the Council, Regulation (EC) no 1907/2006 of the European parliament and of the council of 18 december 2006 concerning the registration, evaluation, authorisation and restriction of chemicals (REACH), establishing a European chemicals agency, amending directive 199, 2006.

[2] European Commission, Commission regulation (EU) No 143/2011 of 17 february 2011 amending annex XIV to regulation (EC) No 1907/2006 of the European parliament and of the council on the registration, evaluation, authorisation and restriction of chemicals ('REACH'), Off. J. Eur. Union L244 (2014) 6–L244/9.

[3] P. Visser, Y. Liu, H. Terryn, J.M.C. Mol, Lithium salts as leachable corrosion inhibitors and potential replacement for hexavalent chromium in organic coatings for the protection of aluminum alloys, J. Coatings Technol. Res. (ISSN: 15470091) 13 (4) (2016) 557–566, http://dx.doi.org/10.1007/s11998-016-9784-6.

[4] P. Visser, H. Terryn, J.M.C. Mol, On the importance of irreversibility of corrosion inhibitors for active coating protection of AA2024-T3, Corros. Sci. (ISSN: 0010938X) 140 (April) (2018) 272–285, http://dx.doi.org/10.1016/j.corsci.2018.05.037.

[5] P. Visser, H. Terryn, J.M.C. Mol, Active corrosion protection of various aluminium alloys by lithium-leaching coatings, Surf. Interface Anal. (ISSN: 10969918) 51 (12) (2019) 1276–1287, http://dx.doi.org/10.1002/sia.6638.

[6] K.A. Yasakau, M.L. Zheludkevich, S.V. Lamaka, M.G. Ferreira, Mechanism of corrosion inhibition of AA2024 by rare-earth compounds, J. Phys. Chem. B (ISSN: 15206106) 110 (11) (2006) 5515–5528, http://dx.doi.org/10.1021/jp0560664.

[7] A.E. Hughes, T.A. Markley, S.J. Garcia, J.M.C. Mol, Comparative study of protection of AA 2024-T3 exposed to rare earth salts solutions, Corros. Eng. Sci. Technol. (ISSN: 17432782) 49 (8) (2014) 674–687, http://dx.doi.org/10.1179/1743278214Y.0000000172.

[8] M. Gobara, A. Baraka, R. Akid, M. Zorainy, Corrosion protection mechanism of Ce4+/organic inhibitor for AA2024 in 3.5% NaCl, RSC Adv. (ISSN: 20462069) 10 (4) (2020) 2227–2240, http://dx.doi.org/10.1039/c9ra09552g.

[9] O. Gharbi, S. Thomas, C. Smith, N. Birbilis, Chromate replacement: what does the future hold? Npj Mater. Degrad. 2 (1) (2018) http://dx.doi.org/10.1038/s41529-018-0034-5.

[10] T.G. Harvey, et al., The effect of inhibitor structure on the corrosion of AA2024 and AA7075, Corros. Sci. (ISSN: 0010938X) 53 (6) (2011) 2184–2190, http://dx.doi.org/10.1016/j.corsci.2011.02.040.

[11] P.A. White, et al., A new high-throughput method for corrosion testing, Corros. Sci. (ISSN: 0010938X) 58 (2012) 327–331, http://dx.doi.org/10.1016/j.corsci.2012.01.016.

[12] D.A. Winkler, et al., Using high throughput experimental data and in silico models to discover alternatives to toxic chromate corrosion inhibitors, Corros. Sci. (ISSN: 0010938X) 106 (2016) 229–235, http://dx.doi.org/10.1016/j.corsci.2016.02.008.

[13] P.A. White, et al., Towards materials discovery: Assays for screening and study of chemical interactions of novel corrosion inhibitors in solution and coatings, New J. Chem. (ISSN: 13699261) 44 (19) (2020) 7647–7658, http://dx.doi.org/10.1039/c9nj06456g.

[14] T.H. Muster, et al., A rapid screening multi-electrode method for the evaluation of corrosion inhibitors, Electrochim. Acta (ISSN: 00134686) 54 (12) (2009) 3402–3411, http://dx.doi.org/10.1016/j.electacta.2008.12.051.

[15] S.J. García, et al., The influence of pH on corrosion inhibitor selection for 2024-T3 aluminium alloy assessed by high-throughput multielectrode and potentiodynamic testing, Electrochim. Acta (ISSN: 00134686) 55 (7) (2010) 2457–2465, http://dx.doi.org/10.1016/j.electacta.2009.12.013.

[16] P.A. White, et al., High-throughput channel arrays for inhibitor testing: Proof of concept for AA2024-T3, Corros. Sci. (ISSN: 0010938X) 51 (10) (2009) 2279–2290, http://dx.doi.org/10.1016/j.corsci.2009.06.038.

[17] B.D. Chambers, S.R. Taylor, High-throughput assessment of inhibitor synergies on aluminum alloy 2024-T3 through measurement of surface copper enrichment, Corrosion (ISSN: 00109312) 63 (3) (2007) 268–276, http://dx.doi.org/10.5006/1.3278353.

[18] D.A. Winkler, et al., Towards chromate-free corrosion inhibitors: Structure-property models for organic alternatives, Green Chem. (ISSN: 14639270) 16 (6) (2014) 3349–3357, http://dx.doi.org/10.1039/c3gc42540a.

[19] E.J. Schiessler, et al., Predicting the inhibition efficiencies of magnesium dissolution modulators using sparse machine learning models, Npj Comput. Mater. (ISSN: 20573960) 7 (1) (2021) 39–41, http://dx.doi.org/10.1038/s41524-021-00658-7.

[20] J. Dai, et al., Cross-category prediction of corrosion inhibitor performance based on molecular graph structures via a three-level message passing neural network model, Corros. Sci. (ISSN: 0010938X) 209 (September) (2022) 110780, http://dx.doi.org/10.1016/j.corsci.2022.110780.

[21] C. Feiler, et al., In silico screening of modulators of magnesium dissolution, Corros. Sci. (ISSN: 0010938X) 163 (September 2019) (2020) 108245, http://dx.doi.org/10.1016/j.corsci.2019.108245.

[22] T.L. Galvão, I. Ferreira, F. Maia, J.R. Gomes, J. Tedim, DATACORTECH: artificial intelligence platform for the virtual screen of aluminum corrosion inhibitors, Npj Mater. Degrad. (ISSN: 23972106) 8 (1) (2024) http://dx.doi.org/10.1038/s41529-024-00489-z.

[23] T.L.P. Galvão, et al., CORDATA : an open data management web application to select corrosion inhibitors, 2022, pp. 4–7, http://dx.doi.org/10.1038/s41529-022-00259-9.

[24] D.A. Winkler, et al., Impact of inhibition mechanisms, automation, and computational models on the discovery of organic corrosion inhibitors, Prog. Mater. Sci. (2024) 101392.

[25] S. Zhao, N. Birbilis, Searching for chromate replacements using natural language processing and machine learning algorithms, Npj Mater. Degrad. (ISSN: 23972106) 7 (1) (2023) http://dx.doi.org/10.1038/s41529-022-00319-0,

[26] P. Taheri, et al., On the importance of time-resolved electrochemical evaluation in corrosion inhibitor-screening studies, Npj Mater. Degrad. (ISSN: 23972106) 4 (1) (2020) 1–4, http://dx.doi.org/10.1038/s41529-020-0116-z.

[27] N. Podobaev, Y.G. Avdeev, Temperature and time effects on the acid corrosion of steel in the presence of acetylenic inhibitors, Prot. Met. 37 (2001) 529–533.

[28] W. Villamizar-Suarez, J. Malo, A. Martinez-Villafañe, J. Chacon-Nava, Evaluation of corrosion inhibitors performance using real-time monitoring methods, J. Appl. Electrochem. 41 (2011) 1269–1277.

[29] J. Sullivan, et al., In situ monitoring of corrosion mechanisms and phosphate inhibitor surface deposition during corrosion of zinc–magnesium–aluminium (ZMA) alloys using novel time-lapse microscopy, Faraday Discuss. 180 (2015) 361–379.

[30] E.C. Roberto, et al., The effect of type of self-assembled system and pH on the efficiency of corrosion inhibition of carbon-steel surfaces, Prog. Org. Coatings 76 (10) (2013) 1308–1315.

[31] V. Vujičić, B. Lovreček, A study of the influence of pH on the corrosion rate of aluminium, Surf. Technol. 25 (1) (1985) 49–57.

[32] H.O. Curkovic, E. Stupnisek-Lisac, H. Takenouti, The influence of pH value on the efficiency of imidazole based corrosion inhibitors of copper, Corros. Sci. 52 (2) (2010) 398–405.

[33] C. Özkan, et al., Laying the experimental foundation for corrosion inhibitor discovery through machine learning, Npj Mater. Degrad. (ISSN: 2397-2106) 8 (1) (2024) 21, http://dx.doi.org/10.1038/s41529-024-00435-z, URL https://www.nature.com/articles/s41529-024-00435-z.

[34] K. Xhanari, et al., Green corrosion inhibitors for aluminium and its alloys: a review, RSC Adv. 7 (44) (2017) 27299–27330.

[35] K. Xhanari, M. Finšgar, Organic corrosion inhibitors for aluminum and its alloys in chloride and alkaline solutions: A review, Arab. J. Chem. (ISSN: 18785352) 12 (8) (2019) 4646–4663, http://dx.doi.org/10.1016/j.arabjc.2016.08.009.

[36] F. Andreatta, L. Fedrizzi, Corrosion inhibitors, in: A.E. Hughes, J.M.C. Mol, M.L. Zheludkevich, R.G. Buchheit (Eds.), Active Protective Coatings, Springer Netherlands, Dordrecht, 2016, pp. 59–84.

[37] P. Visser, et al., The chemical throwing power of lithium-based inhibitors from organic coatings on AA2024-T3, Corros. Sci. (ISSN: 0010938X) 150 (January) (2019) 194–206, http://dx.doi.org/10.1016/j.corsci.2019.02.009.

[38] M. Meeusen, et al., The effect of time evolution and timing of the electrochemical data recording of corrosion inhibitor protection of hot-dip galvanized steel, Corros. Sci. 173 (2020) 108780.

[39] A.M. Homborg, et al., Application of transient analysis using Hilbert spectra of electrochemical noise to the identification of corrosion inhibition, Electrochim. Acta 116 (2014) 355–365.

[40] M.W. Kendig, R.G. Buchheit, Corrosion inhibition of aluminum and aluminum alloys by soluble chromates, chromate coatings, and chromate-free coatings, Corrosion (ISSN: 00109312) 59 (5) (2003) 379–400, http://dx.doi.org/10.5006/1.3277570.

[41] L. Xia, E. Akiyama, G. Frankel, R. McCreery, Storage and release of soluble hexavalent chromium from chromate conversion coatings equilibrium aspects of Cr VI concentration, J. Electrochem. Soc. 147 (7) (2000) 2556.

[42] J. Zhao, et al., Effects of chromate and chromate conversion coatings on corrosion of aluminum alloy 2024-T3, Surf. Coat. Technol. 140 (1) (2001) 51–57.

[43] G.S. Frankel, R.L. McCreery, Inhibition of Al alloy corrosion by chromates, Electrochem. Soc. Interface (ISSN: 1064-8208) 10 (4) (2001) 34–38, http://dx.doi.org/10.1149/2.F06014IF, URL https://iopscience.iop.org/article/10.1149/2.F06014IF.

[44] P. Schmutz, G. Frankel, Influence of dichromate ions on corrosion of pure aluminum and AA2024-T3 in NaCl solution studied by AFM scratching, J. Electrochem. Soc. 146 (12) (1999) 4461.

[45] A.E. Hughes, R. Parvizi, M. Forsyth, Microstructure and corrosion of AA2024, Corros. Rev. (ISSN: 03346005) 33 (1–2) (2015) 1–30, http://dx.doi.org/10.1515/corrrev-2014-0039.

[46] A. Kosari, et al., Dealloying-driven local corrosion by intermetallic constituent particles and dispersoids in aerospace aluminium alloys, Corros. Sci. (ISSN: 0010938X) 177 (July) (2020) 108947, http://dx.doi.org/10.1016/j.corsci.2020.108947.

[47] I. Cole, M. Castillo-Robles, E. De Freitas Martins, P. Ordejón, Molecular modeling applied to corrosion inhibition: a critical review, Npj Mater. Degrad. (ISSN: 2397-2106) 2 (2024) http://dx.doi.org/10.1038/s41529-024-00478-2.

[48] B. Zhou, Y. Wang, Y. Zuo, Evolution of the corrosion process of AA 2024-T3 in an alkaline NaCl solution with sodium dodecylbenzenesulfonate and lanthanum chloride inhibitors, Appl. Surf. Sci. (ISSN: 01694332) 357 (2015) 735–744, http://dx.doi.org/10.1016/j.apsusc.2015.09.093.

[49] M.P. Desimone, G. Gordillo, S.N. Simison, The effect of temperature and concentration on the corrosion inhibition mechanism of an amphiphilic amido-amine in CO2 saturated solution, Corros. Sci. (ISSN: 0010938X) 53 (12) (2011) 4033–4043, http://dx.doi.org/10.1016/j.corsci.2011.08.009.

[50] A. Boag, et al., How complex is the microstructure of AA2024-T3? Corros. Sci. (ISSN: 0010938X) 51 (8) (2009) 1565–1568, http://dx.doi.org/10.1016/j.corsci.2009.05.001.

[51] W. Qafsaoui, M.W. Kendig, S. Joiret, H. Perrot, H. Takenouti, Ammonium pyrrolidine dithiocarbamate adsorption on copper surface in neutral chloride media, Corros. Sci. (ISSN: 0010938X) 106 (2016) 96–107, http://dx.doi.org/10.1016/j.corsci.2016.01.029.

[52] P. Visser, H. Terryn, J.M.C. Mol, Aerospace coatings, in: A.E. Hughes, J.M.C. Mol, M.L. Zheludkevich, R.G. Buchheit (Eds.), Active Protective Coatings, Springer Netherlands, Dordrecht, 2016, pp. 315–372.

[53] M.E. Orazem, B. Tribollet, Electrochemical Impedance Spectroscopy, second ed., John Wiley & Sons, Inc., ISBN: 978-1118527399, 2017.

[54] A.J. Bard, L.R. Faulkner, H.S. White, Electrochemical Methods: Fundamentals and Applications, third ed., John Wiley & Sons, 2022.

[55] H. Yasuda, Q. Yu, M. Chen, Interfacial factors in corrosion protection: an EIS study of model systems, Prog. Org. Coatings (ISSN: 03009440) 41 (4) (2001) 273–279, http://dx.doi.org/10.1016/S0300-9440(01)00142-4, URL https://linkinghub.elsevier.com/retrieve/pii/S0300944001001424.

[56] A.C. Lazanas, M.I. Prodromidis, Electrochemical impedance spectroscopy a tutorial, ACS Meas. Sci. Au (ISSN: 2694250X) 3 (3) (2023) 162–193, http://dx.doi.org/10.1021/acsmeasuresciau.2c00070.

[57] P. Visser, M. Meeusen, Y. Gonzalez-Garcia, H. Terryn, J.M.C. Mol, Electrochemical evaluation of corrosion inhibiting layers formed in a defect from lithium-leaching organic coatings, J. Electrochem. Soc. (ISSN: 0013-4651) 164 (7) (2017) C396–C406, http://dx.doi.org/10.1149/2.1411707jes.

[58] I. Mohammadi, T. Shahrabi, M. Mahdavian, M. Izadi, Cerium/diethyldithiocarbamate complex as a novel corrosion inhibitive pigment for AA2024-T3, Sci. Rep. (ISSN: 20452322) 10 (1) (2020) 1–15, http://dx.doi.org/10.1038/s41598-020-61946-8.

[59] N.C. Rosero-Navarro, et al., Optimization of hybrid sol-gel coatings by combination of layers with complementary properties for corrosion protection of AA2024, Prog. Org. Coatings (ISSN: 03009440) 69 (2) (2010) 167–174, http://dx.doi.org/10.1016/j.porgcoat.2010.04.013.

[60] C.H. Hsu, F. Mansfeld, Technical note: Concerning the conversion of the constant phase element parameter Y 0 into a capacitance, CORROSION (ISSN: 0010-9312) 57 (9) (2001) 747–748, http://dx.doi.org/10.5006/1.3280607, URL https://meridian.allenpress.com/corrosion/article/57/9/747/161974/Technical-Note-Concerning-the-Conversion-of-the.

[61] E. Barsoukov, J.R. Macdonald, Impedance Spectroscopy: Theory, Experiment, and Applications, second ed., John Wiley & Sons, Inc., ISBN: 0471-64749-7, 2005.

[62] L. Kwiatkowski, M. Grobelny, P. Konarski, Selection of processing parameters for the conversion coatings on high-strength aluminum alloys by cyclic voltammetry, Mater. Sci. 50 (2015) 634–645.

[63] R. Williams, pKa values in water compilation, ACS Org. Div. (2022) URL https://organicchemistrydata.org/hansreich/resources/pka/pka_data/pka-compilation-williams.pdf.

[64] N. Saeidi, F. Harnisch, V. Presser, F.D. Kopinke, A. Georgi, Electrosorption of organic compounds: State of the art, challenges, performance, and perspectives, Chem. Eng. J. (ISSN: 13858947) 471 (June) (2023) 144354, http://dx.doi.org/10.1016/j.cej.2023.144354.

[65] C. Laurent, F. Scenini, T. Monetta, F. Bellucci, M. Curioni, The contribution of hydrogen evolution processes during corrosion of aluminium and aluminium alloys investigated by potentiodynamic polarisation coupled with real-time hydrogen measurement, Npj Mater. Degrad. (ISSN: 23972106) 1 (1) (2017) 1–7, http://dx.doi.org/10.1038/s41529-017-0011-4.

[66] L. Kwiatkowski, M. Grobelny, P. Konarski, Selection of processing parameters for the conversion coatings on high-strength aluminum alloys by cyclic voltammetry, Mater. Sci. (ISSN: 1573885X) 50 (5) (2015) 13–22, http://dx.doi.org/10.1007/s11003-015-9765-4.